Journal of Electromagnetic Waves and Applications, Vol. 14, 233–248, 2000

SIMULATING BISTATIC SCATTER FROM SURFACES COVERED WITH VEGETATION

P. Ferrazzoli, L. Guerriero, and D. Solimini

Dipartimento di Informatica, Sistemi e Produzione
Università Tor Vergata
Via di Tor Vergata, 00133 Roma, Italy

Abstract–Many experimental and theoretical studies have shown that the use of active systems for monitoring plant biomass suffers from saturation problems. The possibility of overcoming this limit by considering a bistatic configuration is theoretically analyzed for the case of sunflower fields. An electromagnetic model, already developed and validated on active and passive data, has been modified to yield the bistatic scattering coefficient. To this end, coherent scattering from the soil has been included, which resulted to be the most relevant component of specular scattering. According to model simulations, the specular scattering cross section normalized to area does not exhibit severe saturation effects and shows a better sensitivity to biomass at higher frequencies.

1. INTRODUCTION

Monitoring vegetation biomass is one of the relevant applications that remote sensing could find both in ecology [1] and in agriculture [2]. Major applications include, on one side, forestry inventory and deforestation monitoring, and, on the other, crop monitoring, yield estimates, and harvest control. Both their almost all-weather capability and enhanced spatial resolution make imaging radars apt to these tasks.

A number of radar experiments, including spaceborne and airborne SAR, have been carried out to demonstrate a significant correlation of backscattering at different polarizations and frequencies to tree [3–7] or crop [8–13] biomass. The information contained in amplitude and phase of the radar returns makes the retrieval of the vegetation biomass feasible, in principle, by inverting backscattering data. Esti-

mates have been carried out by implementing a variety of techniques, including multiple regressions [3, 6, 14–17], empirical or theoretical algorithms [12, 18], possibly exploiting coherence [19], and neural networks [20–24]. The reported results are generally promising in view of obtaining quantitative information on the vegetation parameters and, in particular, on its biomass. However, both the experience gained from the various projects and theoretical results seem to indicate that a major limit to the actual use of radar in this field exists, due to the early saturation of its response with respect to plant biomass [11, 25]. Among the remedies to overcome this drawback, the use of stepped algorithms, which estimate primary variates for structural classes of forested areas [18] and of neural networks, which have the potential of fully exploiting the multi-dimensionality of the measurement space [26], have been suggested. Although these retrieval techniques can provide powerful means of extracting the biomass information embedded in multi-frequency multi-polarization measurements, devising radar configurations which by themselves have the potential of yielding a higher sensitivity, can be appropriate. Recently, the possible use of a bistatic radar configuration has been considered and theoretically analyzed with the intent of widening the biomass range over which an appreciable radar dynamics is maintained [27]. Such a technique could use a parasitic SAR system based on a non-co-operative illuminator [28], like, for example, a geostationary transmitter and a geosynchronous receiver, as suggested in [29].

Within the general purpose of retrieving the plant biomass, this contribution discusses the relevant features of bistatic scattering from vegetation, on the basis of a simulation analysis carried out using the fully polarimetric theoretical model developed at Tor Vergata [30, 31]. The case of sunflower plants has been chosen as representative of a large class of vegetation, composed of nearly vertical stalks bearing an upper canopy of stems and planar leaves. The analysis can be readily extended to other types of agricultural crops and forests, by tuning the vegetation parameters and possibly including the appropriate growth models.

The normalized scattering cross sections in the specular direction have been calculated at L- and C-band and compared with the backscattering coefficients computed for the same canopies. For a deeper understanding of the involved scattering mechanisms, the contributions coming from the various components of the canopy and from the

underlying soil have been evidentiated and discussed. The linear co-polar ($\sigma^0_{hh}, \sigma^0_{vv}$) and cross-polarized ($\sigma^0_{hv}$) cases have been considered in detail, but a fully polarimetric analysis has been carried out too. The enhancement of sensitivity with respect to the monostatic case has been noted and its outcome in terms of predicted improvement in the retrieval of biomass is briefly discussed.

2. THE MODEL

The electromagnetic scattering and emission model for vegetated terrain developed at Tor Vergata University considers the vegetation-soil system as a canopy of discrete lossy scatterers overlying a homogeneous lossy half-space with rough interface. Dielectric elements of simple shape, such as discs and cylinders, are assumed: discs represent planar leaves, while cylinders represent trunks, branches, stems and needles. In order to represent a sunflower field, three main canopy components have been identified, as sketched in fig. 1.

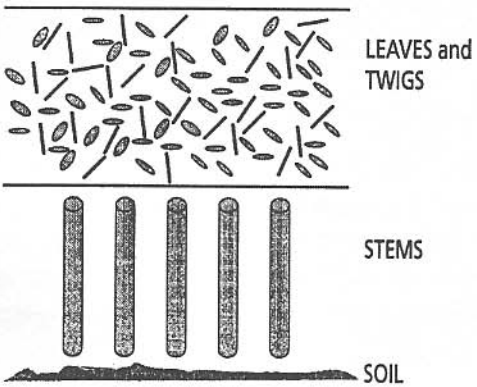

Figure 1. Sketch of model representation for sunflower crops.

- the top layer, filled by twigs and leaves;
- an intermediate layer containing near vertical cylinders representing stalks;
- the bottom layer, representing soil.

The electromagnetic properties of the lossy scatterers, which model the plant constituents, are described by their extinction cross section and by their bistatic scattering cross section, which is a function of the

incident (θ, ϕ) and scattering (θ_s, ϕ_s) directions represented in fig. 2. These quantities are computed using the proper approximation, according to the object dimension and wavelength under consideration. Once the above indicated quantities are known, the different contributions of the top layer scatterers are combined by means of the Matrix Doubling algorithm, which is also applied to include contributions from the soil. Details about the simulation technique, and about the approximations used to model the electromagnetic behaviour of discs, cylinders and of the soil can be found in [31–33]. In those papers, comparisons with experimental results are also shown, which validate the model both in its active and its passive form.

The bistatic scattering coefficient $\sigma^{\circ}_{pq}(\theta, \theta_s, \phi, \phi_s)$ is composed of two contributions: an incoherent scattering term $\sigma^{\circ i}_{pq}(\theta, \theta_s, \phi, \phi_s)$, and a coherent one $\sigma^{\circ c}_{pq}(\theta, \theta_s, \phi, \phi_s)$ (where p and q are the polarizations of the scattered and incident waves).

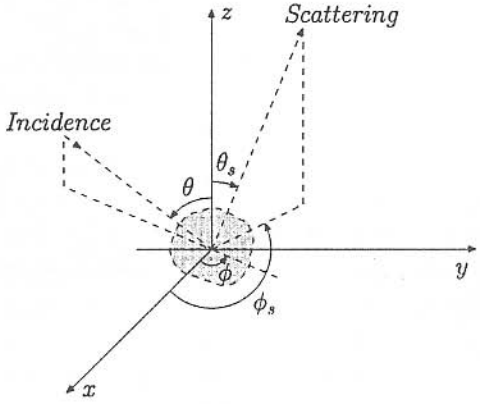

Figure 2. Scatterer reference system: $\theta =$ off-normal angle of incidence, $\theta_s =$ off-normal angle of scattering; $\phi =$ azimuth angle of incidence, ϕ_s = azimuth angle of scattering.

In the monostatic case $(\theta = \theta_s, \phi_s = \phi + \pi)$, the backscattering coefficient of the whole canopy system is:

$$\sigma^{\circ b}_{pq}(\theta) = \sigma^{\circ bi}_{pq}(\theta) + \sigma^{\circ bc}_{pq}(\theta)$$

The first term includes direct backscatter from the soil, the top layer, and multiple scattering effects between them; the second term represents the soil-stalk specular reflection ("corner effect").

When considering scattering in the specular direction ($\theta = \theta_s, \phi_s = \phi$), there is no soil-stalk corner effect, but coherent scattering from the soil in the specular direction must be taken into account. Therefore, also in this case the scattering coefficient is made up of two terms:

$$\sigma^{os}_{pq}(\theta) = \sigma^{osi}_{pq}(\theta) + \sigma^{osc}_{pq}(\theta)$$

As pointed out in [31] and [32], the scattering properties of the top layer-soil system are described by the Fourier components of a scattering function $S_{mpq}(\theta, \theta_s)$, where m is the order of the Fourier components, which represent the dependence on the azimuth angle $\phi_s - \phi$. The incoherent bistatic scattering coefficient results to be proportional to the sum of the Fourier series:

$$\sigma^{oi}_{pq}(\theta, \theta_s, \phi, \phi_s) = \alpha \sum_m S_{mpq}(\theta, \theta_s) \cos(m(\phi_s - \phi)) \qquad (1)$$

with α as a proportionality constant.

In the monostatic case, we have:

$$\sigma^{obi}_{pq}(\theta) = \alpha \sum_m S_{mpq}(\theta, \theta) \cos(m\pi)$$

and

$$\sigma^{obc}_{pq}(\theta) = T_{qq}(\theta)\sigma^{o}_{sgpq}(\theta)T_{pp}(\theta)$$

where σ^{o}_{sgpq} represents the stalk-ground double bounce contribution which is attenuated by the stalks themselves and by the overlying top layer (T represents the overall transmissivity).

In the specular configuration $\phi_s - \phi = 0$, so that:

$$\sigma^{osi}_{pq}(\theta) = \alpha \sum_m S_{mpq}(\theta, \theta)$$

while

$$\sigma^{osc}_{pq}(\theta) = T_{qq}(\theta, \theta)\sigma^{oc}_{pq}(\theta, \theta, \phi, \phi)T_{pp}(\theta, \theta)$$

$\sigma^{oc}_{pq}(\theta, \theta, \phi, \phi)$ is the coherent scattering coefficient of the soil, in the specular direction. Also in this case, attenuation by the overlying vegetation is introduced by means of the transmissivity T.

The coherent scattering coefficient $\sigma^{oc}_{pq}(\theta, \theta, \phi, \phi)$ has been computed using the expression given in [34], where the soil specular reflection Müller matrix [31] has been inserted in order to get the polarimetric contribution. In [34] the coherent scattering coefficient was shown

to depend not only on surface roughness, but also on the system configuration (pixel dimension and radar height). The simulations carried out in this paper refer to system parameters typical of ERS satellite.

2.1 Model Inputs

The vegetation and soil parameters used to model sunflower bistatic scattering have been mostly derived by ground measurements collected in Tuscany during the MAC Europe 91 campaign. Details are given in [11] and [31].

The top layer parameters are:

- Disc (leaf) thickness: $\delta = 0.025\,\mathrm{cm}$
- Disc radius: $a_D = 8\,\mathrm{cm}$
- Inclined cylinder (stem) radius: $a_C = 0.25\,\mathrm{cm}$
- Inclined cylinder length: $\ell_C = 20\,\mathrm{cm}$
- Leaf and stem moisture content (by weight): 85%
- Leaf and stem orientation distribution:
  $0 < \alpha < 2\pi,\ p(\alpha) = 1$
  $0 < \beta < \pi/2,\ p(\beta) = 1$
  $\gamma = 0$

At the higher frequencies, since the effects of bending and corrugation become important, we have subdivided each leaf into several circular discs whose diameter has been put equal to half a wavelength.

The stalk layer parameters are:

- Stalk density: $N_s = 7.9\,\mathrm{m}^{-2}$
- Stalk moisture content (by weight): 90%

The soil parameters are:

- Soil roughness standard deviation: $\sigma_z = 1.25\,\mathrm{cm}$
- Soil roughness average slope: $m_s = 0.3$
- Volumetric soil moisture: $m_V = 17.5\%$

Computations have been carried out for several values of Plant Water Content PWC (kg/m^2), which is a significant crop biomass indicator. Some empirical relationships have been found for the following parameters:

- LAI (Leaf Area Index)$=0.9 \times$ PWC
- Stalk height (cm): $h_s = \begin{cases} 0.75(60 - 10 \times \mathrm{LAI}) \times \mathrm{LAI} & (\mathrm{LAI} < 3) \\ 0.75 \times 30 \times \mathrm{LAI} & (\mathrm{LAI} > 3) \end{cases}$
- Stalk radius (cm): $a_s = 0.75 + 0.125 \times \mathrm{LAI}$

3. THEORETICAL RESULTS

To illustrate the relevant features and the potential of the bistatic technique in monitoring the biomass of agricultural crops, simulations have been conducted at L (1.2 GHz) and C (5.3 GHz) band for an observation angle of 45° . In fig. 3, the computed scattering cross-section, normalized to area, of the sunflower canopy in the specular direction is reported as a function of the Plant Water Content (PWC). For ease of comparison, in fig. 3 the backscattering coefficient modeled for the same canopy and for the same frequencies, is also reported. These plots show that the biomass dependency of radar backscatter varies as a function of radar wavelength and polarization reaching saturation after a certain biomass level. In general it can be noted that, in the monostatic case, HV polarization is the most sensitive to biomass, and that the saturation point is higher for longer wavelength.

In the bistatic configuration, the co-polar responses show a decreasing trend with increasing PWC, without appreciable saturation effect even at the largest biomass values. Furthermore, a larger dynamic range is also apparent: about 20 dB at L-Band in vertical polarization, becoming more than 40 dB at C-Band. The normalized specular cross section in HV polarization is not reported since its values and trend vs PWC are very close to the backscattering case, being null the theoretical soil coherent component.

To get an insight into the bistatic scattering mechanisms, the various contributions coming from the canopy components are reported in fig. 4. (Note that in these plots a larger ordinate scale has been used, in order to incorporate all contributions). The simulation results in fig. 4 indicate that scattering in the specular direction is dominated by the soil coherent component, since all incoherent contributions are several dB's lower than total specular scattering. Hence, the sensitivity to biomass is connected to the increasing attenuation by the plant canopy, which reduces the coherent scattering from the soil.

The results reported in fig. 4 refer to L-Band, but analogous considerations apply to C-Band. At higher frequencies, attenuation introduced by vegetation is larger, leading to a steeper curve of σ^{os} vs PWC.

Since specular reflection is instrumental to the extraction of biomass information, those effects that quench specularity are detrimental to the proposed technique. The impact of soil roughness on the coherent component increases with frequency: at C-band the specular reflection

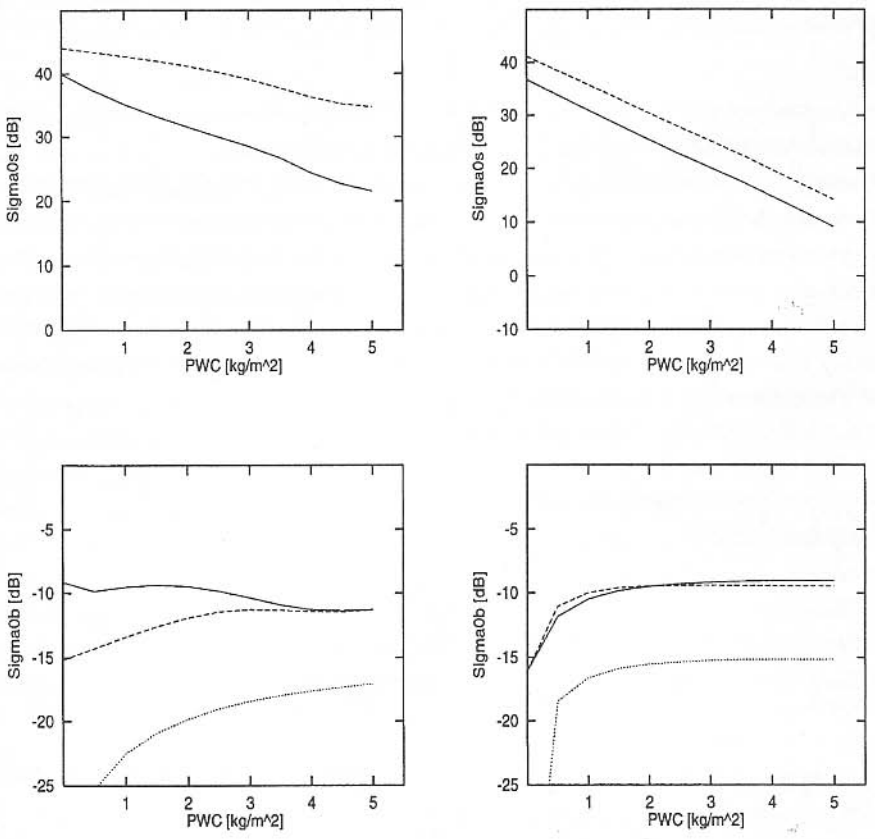

Figure 3. Normalized scattering cross-section in the specular direction (top line) and backscattering coefficient (bottom line) of sunflower vs. PWC. Continuous line is VV polarization, dashed line is HH, dotted line is HV. Frequency is $f = 1.2\,\mathrm{GHz}$ (left row) and 5.3 GHz (right row). Incidence angle $\theta = 45°$. Vegetation and soil parameters are listed in section 2.1.

is cut down by a height standard deviation higher than about 2 cm, whereas at L-band only a moderate decrease ($\approx 10\,\mathrm{dB}$) of the coherent component can be observed for σ_z up to 5 cm. On its side, the extension of the surface that could be monitored from a single location of the satellite pair by exploiting the specular bistatic technique is limited by the degree of specularity of the reflection. Indeed, reflection and incidence angles coincide for a single pixel, while their difference increases when the observed region is moved from the central location

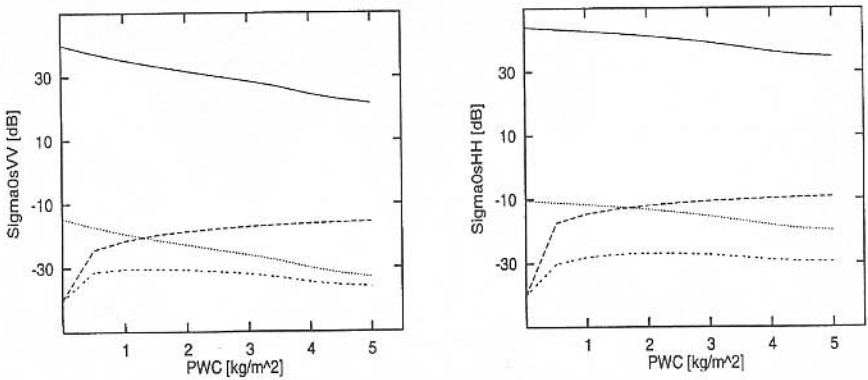

Figure 4. Components of the normalized scattering cross-section in the specular direction: VV polarization (left), HH polarization (right). $f = 1.2\,\mathrm{GHz}$, $\theta = 45°$. Continuous line is the soil coherent scattering component; dotted line is the soil incoherent scattering component; dashed line is the top layer component; double dashed line is the top layer-soil interaction component.

(fig. 5). To appreciate the sensitivity of the proposed bistatic approach to the degree of specularity, the incidence angle, and consequently the observation angle, have been moved off $\theta = 45°$. This corresponds to observe a pixel at a distance $L = \frac{H\Delta\theta}{\cos^2\theta}$ from the purely specular one (H is the system altitude, and $\Delta\theta$ is the variation in the incidence angle. A flat earth is assumed). In fig. 6 the bistatic scattering coefficient is reported as a function of PWC for various distances. For L-band bistatic observation from an altitude $H = 800\,\mathrm{km}$, an appreciable sensitivity to vegetation biomass is maintained up to distances $L \simeq 13\,\mathrm{km}$ (i.e., up to an off-specular angle $\Delta\theta \simeq 0.5°$), thus allowing monitoring a strip 26 km wide. Increasing frequency rapidly degrades the sensitivity of off-specular scattering to vegetation biomass: at C-band the expected width of the observable area, in which sensitivity to PWC up to 3 $\mathrm{kg/m^2}$ is still appreciable, reduces to less than 6 km.

Finally, in fig. 7 the polarimetric signature of a sunflower field with a PWC=3.5 $\mathrm{kg/m^2}$ has been simulated, both in the bistatic and monostatic configurations. The polarimetric signatures exhibit apparent differences in the two configurations. Some peculiarities of the monostatic case are more evidentiated in the bistatic case: like the difference between horizontal and vertical polarization, the difference between co- and cross-polar circular polarizations, and the maximum at linear

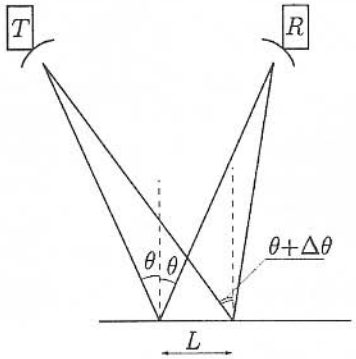

Figure 5. Bistatic system in an off-specular configuration. $\theta + \Delta\theta$ is the incidence angle, L is the distance from the pixel observed under perfect specularity.

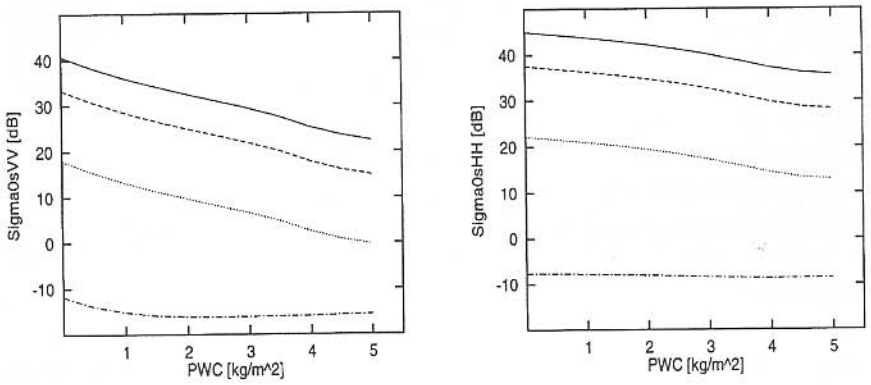

Figure 6. Normalized scattering cross-section in the off-specular direction: VV polarization (left), HH polarization (right). $f = 1.2$ GHz. Continuous line: specular scattering; dashed line: bistatic scattering from a pixel with $L = 5$ Km; dotted line: scattering from a pixel with $L = 10$ Km; dot-dashed line: scattering from a pixel with $L = 15$ Km.

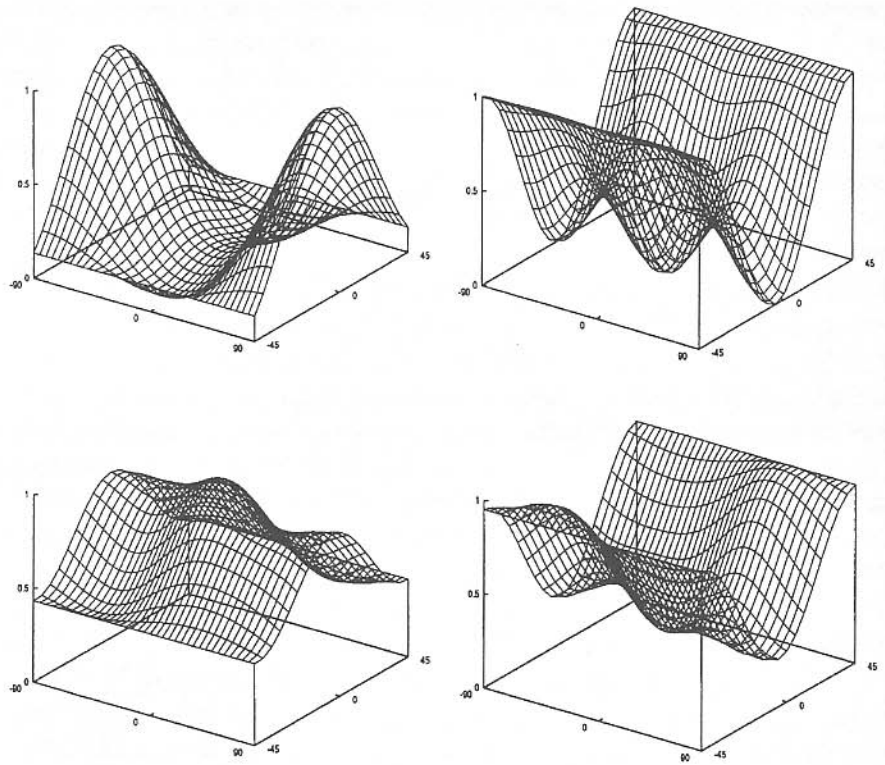

Figure 7. Theoretical polarimetric signatures of a sunflower field with PWC = 3.5 kg/m^2. f = 1.2 GHz, $\theta = 45°$. Top line: bistatic configuration, bottom line: monostatic configuration. Left row: co-polar signature, right row: cross-polar signature.

cross-polarization with 45 ° inclination. These results indicate that bistatic data can add information in polarimetric applications, like for example vegetation classification.

4. CONCLUSIONS

It is now becoming possible to perform radar bistatic measurements by using systems deployed for other purposes, like positioning or broadcasting satellites. The use of non-co-operative radar illuminators would reduce the cost of bistatic operation and would make it more affordable by the remote sensing community. Since the scattering cross-section is

sensitive to the geometry of the measurement system and, in particular, to the incidence and scattering angles, such a radar configuration may have the potential of providing data which, for some applications, have better characteristics with respect to the monostatic case. Here we have considered the problem of plant biomass monitoring, which suffers from the early saturation of the backscattering coefficients. To this end, the performance of a bistatic radar in a specular configuration has been simulated to investigate its expected capability of widening the range of biomass over which significant measures can be taken. A numerical model simulating the bistatic normalized scattering section of a sunflower crop has been run and the results have been compared with those obtained for the same canopy in the monostatic case. The most important differences are essentially due to the specular coherent reflection from the soil, which appears to be the dominant component in the scattering process. Hence, the attenuation by the vegetation becomes the main mechanism through which the bistatic radar response depends on the biomass. The reported results indicate that such a bistatic system would maintain an appreciable sensitivity to the PWC of crops over a considerably wider range than in the monostatic operation. From this point of view, C-band would be preferable to L-band, whose attenuation is considerably less sensitive to agricultural vegetation. Similar results can be found for forests, however, it should be pointed out that the roughness of a forest floor is frequently sufficiently high to substantially reduce the specular component. Moreover, a growth model of a natural pine stand [35] points out a decrease of the number of trees per unit area with increasing woody biomass. As shown by our simulations (results not reported here), this ends up in a weaker dependence of the attenuation and, in turn, of the measured scattering, on the biomass. Hence, the advantage that a bistatic configuration could offer over the monostatic one is expected to become less distinct in case of forests, at least for some types of natural stands.

ACKNOWLEDGMENT

Keen comments by an anonymous reviewer are gratefully acknowledged. This work has been partially supported by ASI, Agenzia Spaziale Italiana.

REFERENCES

1. Bretherton, F. P., "Earth system science and remote sensing," *Proc. IEEE,* Vol. 73, 1118–1127, 1985.
2. Bernard, A. C., and J. Meyer-Roux, eds., *Proc. Conf. The MARS Project: Overview and Perspectives,* Office for Official Publications of the European Communities, Cat. N. CL-NA-15599-EN-C, Luxembourg, 1994.
3. Le Toan, T., A. Beaudoin, J. Riom, and D. Guyon, "Relating forest biomass to SAR data," *IEEE Trans. Geosci. Remote Sensing,* Vol. 30, 403–411, 1992.
4. Dobson, M. C., F. T. Ulaby, T. Le Toan, A. Beaudoin, E. S. Kasischke, and N. L. Christensen, Jr., "Dependence of radar backscatter on coniferous forest biomass," *IEEE Trans. Geosci. Remote Sensing,* Vol. 30, 643–659, 1992.
5. Kasischke, E. S., L. L. Bourgeau-Chavez, N. L. Christensen, Jr., and E. Haney, "Observations on the sensitivity of ERS-1 SAR image intensity to changes in aboveground biomass in young loblolly pine forests," *Int. J. Remote Sensing,* Vol. 15, 3–16, 1994.
6. Ranson, K. J., S. Saatchi, and G. Sun, "Boreal forest echosystem characterization with SIR-C/X-SAR," *IEEE Trans. Geosci. Remote Sensing,* Vol. 33, 867–876, 1995.
7. Askne, J. I. H., P. B. G. Dammert, L. M. H. Ulander, and G. Smith, "C-band repeat-pass interferometric observations of the forest," *IEEE Trans. Geosci. Remote Sensing,* Vol. 35, 25–35, 1997.
8. Le Toan, T., H. Laur, E. Mougin, and A. Lopes, "Multitemporal and dual polarization observations of agricultural vegetation covers by X-band SAR images," *IEEE Trans. Geosci. Remote Sensing,* Vol. 27, 709–718, 1989.
9. Bouman, B. A. M., "Crop parameter estimation from ground-based X-band (3-cm wave) radar backscattering data," *Remote Sens. Environ.,* Vol. 37, 193–205, 1991.
10. Bouman, B. A. M., and D. H. Hoekman, "Multi-temporal, multi-frequency radar measurements of agricultural crops during the Agriscatt-88 campaign in the Netherlands," *Int. J. Remote Sensing,* Vol. 14, 1595–1614, 1993.
11. Ferrazzoli, P., S. Paloscia, P. Pampaloni, G. Schiavon, S. Sigismondi, and D. Solimini, "The potential of multifrequency polarimetric SAR in assessing agricultural and arboreous biomass," *IEEE Trans. Geosci. Remote Sensing,* Vol. 35, 5–17, 1997.
12. Le Toan, T., F. Ribbes, L.-F. Wang, N. Floury, K.-H. Ding, J. A. Kong, M. Fujita, and T. Kurosu, "Rice crop mapping and monitoring using ERS-1 data based on experiment and modeling

results," *IEEE Trans. Geosci. Remote Sensing,* Vol. 35, 41–56, 1997.

13. Moran, M. S., A. Vidal, D. Troufleau, Y. Inoue, and T. A. Mitchell, "Ku- and C-band SAR for discriminating agricultural crop and soil conditions," *IEEE Trans. Geosci. Remote Sensing,* Vol. 36, 265–272, 1998.
14. Beaudoin, A., T. Le Toan, S. Goze, E. Nezry, A. Lopes, E. Mougin, C. C. Hsu, H. C. Han, J. A. Kong, and R. T. Shin, "Retrieval of forest biomass from SAR data," *Int. J. Remote Sensing,* Vol. 15, 2777–2796, 1994.
15. Polatin, P. F., K. Sarabandi, and F. T. Ulaby, "An iterative inversion algorithm with application to the polarimetric radar response of vegetation canopies," *IEEE Trans. Geosci. Remote Sensing,* Vol. 32, 62–71, 1994.
16. Rignot, E., J. B. Way, C. Williams, and L. Viereck, "Radar estimates of aboveground biomass in boreal forests of interior Alaska," *IEEE Trans. Geosci. Remote Sensing,* Vol. 32, 1117–1124, 1994.
17. Kasischke, E. S., N. L. Christensen, Jr., and L. L. Bourgeau-Chavez, "Correlating radar backscatter with components of biomass in loblolly pine forest," *IEEE Trans. Geosci. Remote Sensing,* Vol. 33, 643–659, 1995.
18. Dobson, M. C., F. T. Ulaby, L. E. Pierce, T. L. Sharik, K. M. Bergen, J. Kellndorfer, J. R. Kendra, E. Li, Y. C. Lin, A. Nashashibi, K. Sarabandi, and P. Siqueira, "Estimation of forest biophysical characteristics in Northern Michigan with SIR-C/X-SAR," *IEEE Trans. Geosci. Remote Sensing,* Vol. 33, 877–894, 1995.
19. Wegmüller, U. and C. Werner, "Retrieval of vegetation parameters with SAR interferometry," *IEEE Trans. Geosci. Remote Sensing,* Vol. 35, 18–24, 1997.
20. Dawson, M. S., J. Olvera, A. K. Fung, and M. T. Manry, "Inversion of surface parameters using fast learning neural networks," *Proc. IGARSS'92,* 910–912, 1992.
21. Pierce, L. E., K. Sarabandi, and F. T. Ulaby, "Application of an artificial neural network in canopy scattering inversion," *Int. J. Remote Sensing,* Vol. 15, 3263–3270, 1994.
22. Dawson, M. S., "Applications of electromagnetic scattering models to parameter retrieval and classification," A. K. Fung, ed., *Microwave Scattering and Emission Models and their Applications,* Chapt. 12, Artech House, Norwood, MA, 1994.
23. Del Frate, F., G. Schiavon, and D. Solimini, "Neural network inversion of SAR data to retrieve vegetation parameters," *Int.*

Symp. Retrieval of bio- and geophysical parameters from SAR data for land applications, 19–26, Toulouse, France, October 10-13, 1995.

24. Xiao, R., R. Carande, and D. Ghiglia, "A neural network approach for tree height estimation using IFSAR data," *Proc. IGARSS'98,* 1565–1567, 1998.
25. Imhoff, M. L., "Radar backscatter and biomass saturation: ramifications for global biomass inventory," *IEEE Trans. Geosci. Remote Sensing,* Vol. 33, 510–518, 1995.
26. Del Frate, F., and D. Solimini, "Retrieving forest biomass from SAR data inverted by a neural network algorithm," *Second Int. Symp. Retrieval of Bio- and Geophysical Parameters from SAR Data for Land Applications,* Noordwijk, Netherlands, October 21-23, 1998.
27. Ferrazzoli, P., L. Guerriero, and D. Solimini, "Comparison between predicted performances of bistatic and monostatic radar in vegetation monitoring," *Proc. of IGARSS'94,* 1850–1852, Pasadena, CA, Aug. 1994.
28. Dunsmore, M. R. B., "Bistatic Radars," *Advanced Radar Techniques and Systems,* G. Galati, ed., 822–920, Peter Peregrinus, Stevenage, U.K., 1993.
29. Prati, C., F. Rocca, D. Giancola, and A. Monti Guarnieri, "Passive geosynchronous SAR system reusing backscattered digital audio broadcasting signals," *IEEE Trans. Geosci. Remote Sensing,* Vol. 36, 1973–1976, 1998.
30. Ferrazzoli, P., L. Guerriero, and D. Solimini, "Numerical model of microwave backscattering and emission from terrain covered with vegetation," *J. Applied Computational Electromagnetics Soc.,* Vol. 6, 175–191, 1991.
31. Bracaglia, M., P. Ferrazzoli, and L. Guerriero, "A fully polarimetric multiple scattering model for crops," *Remote Sens. Environ.,* Vol. 54, 170–179, 1995.
32. Ferrazzoli, P., and L. Guerriero, "Radar sensitivity to tree geometry and woody volume: A model analysis," *IEEE Trans. Geosci. Remote Sensing,* Vol. 33, 360–371, 1995.
33. Ferrazzoli, P., and L. Guerriero, "Modeling microwave emission from vegetation covered surfaces: a parametric analysis," *Passive Microwave Remote Sensing of Land-Atmosphere Interactions,* B. J. Choudhury, Y. H. Kerr, E. G. Njoku, and P. Pampaloni, eds., 389–402, VSP, Utrecht, NL, 1995.
34. Fung, A. K., and H. J. Eom, "Coherent scattering of a spherical wave from an irregular surface," *IEEE Trans. Antennas Propagat.,* Vol. AP31, 68–72, 1983.

35. Kasischke, E. S., N. L. Christensen, Jr., and E. M. Haney, "Modeling of geometric properties of loblolly pine tree and stand characteristics for use in radar backscatter studies," *IEEE Trans. Geosci. Remote Sensing,* Vol. 32, 800–821, 1994.

Paolo Ferrazzoli graduated from the University "La Sapienza" of Rome in 1972. In 1974 he joined Telespazio s.p.a., where he was mainly active in the fields of antennas, slant-path propagation and advanced satellite telecommunication systems. In 1984 he joined "Tor Vergata" University of Rome, where he is presently working, teaching Microwaves. His research, here, concerns propagation and microwave remote sensing of vegetated terrains, with particular emphasis on electromagnetic modeling. He has been involved in international experimental remote sensing campaigns such as AGRISAR AGRISCATT, MAESTRO-1, MAC-Europe and SIR-C/X-SAR. He is a member of the Science Team of the SMOS Project.

Leila Guerriero received the Laurea degree in Physics in 1986 and the Ph.D. degree in Electromagnetism in 1991. She has been a Permanent Researcher at "Tor Vergata" University, Rome, Italy, since 1994, where she is mainly concerned with modeling microwave backscattering and emissivity from agricultural and forested areas. In 1988, she was involved in a cooperation between the Jet Propulsion Laboratory Pasadena, CA, and the Italian National Research Council for investigations on geophysical applications of imaging spectrometry in infrared and visible remote sensing.

Domenico Solimini has been associated with the Department of Electrical Engineering of the University of Rome since 1963, and is currently a Full Professor at the Tor Vergata University, Rome. Since 1966 he has taught courses on antennas and propagation, remote sensing, and electromagnetic fields. His research activity has been concerned with nonlinear electromagnetics, microwave antennas, microwave and millimeter-wave propagation, and remote sensing. In this field, he has been involved in several international projects.